

Cell Reports, Volume 42

Supplemental information

**FTY720 requires vitamin B₁₂-TCN2-CD320 signaling
in astrocytes to reduce disease
in an animal model of multiple sclerosis**

Deepa Jonnalagadda, Yasuyuki Kihara, Aran Groves, Manisha Ray, Arjun Saha, Clayton Ellington, Hyeon-Cheol Lee-Okada, Tomomi Furihata, Takehiko Yokomizo, Edward V. Quadros, Richard Rivera, and Jerold Chun

Supplemental Data

FTY720 requires vitamin B₁₂-TCN2-CD320 signaling in astrocytes to reduce disease in an animal model of multiple sclerosis

Authors: Deepa Jonnalagadda^{1,†}, Yasuyuki Kihara^{1,†,*}, Aran Groves^{1,2,†}, Manisha Ray¹, Arjun Saha³, Clayton Ellington¹, Hyeon-Cheol Lee-Okada⁴, Tomomi Furihata⁵, Takehiko Yokomizo⁴, Edward V. Quadros⁶, Richard Rivera¹, Jerold Chun^{1,*}

This file contains the following supplementary figures.

Fig. S1. snRNA-seq and CD320 identification.

Fig. S2. Analyses of B₁₂^{def} EAE mice and B₁₂^{free} astrocytes.

Fig. S3. FTY720 efficacy in B₁₂^{def} mice.

Fig. S4. CIR-based binding assay and CD320 internalization.

***Table S1.** DEGs of nuclear RNA-seq, corresponding to Fig. 1C

***Table S2.** Reactome pathway analysis¹ of Cluster I genes that were commonly up-regulated in S1P₁-AsCKO^{fos} and FTY720-treated groups as compared to WT^{fos}.

***Table S3.** DEGs of astrocyte RNA-seq, corresponding to Fig. 2D.

***Table S4.** Primer sets.

*Supplemental tables are provided in an Excel spreadsheet in a different file.

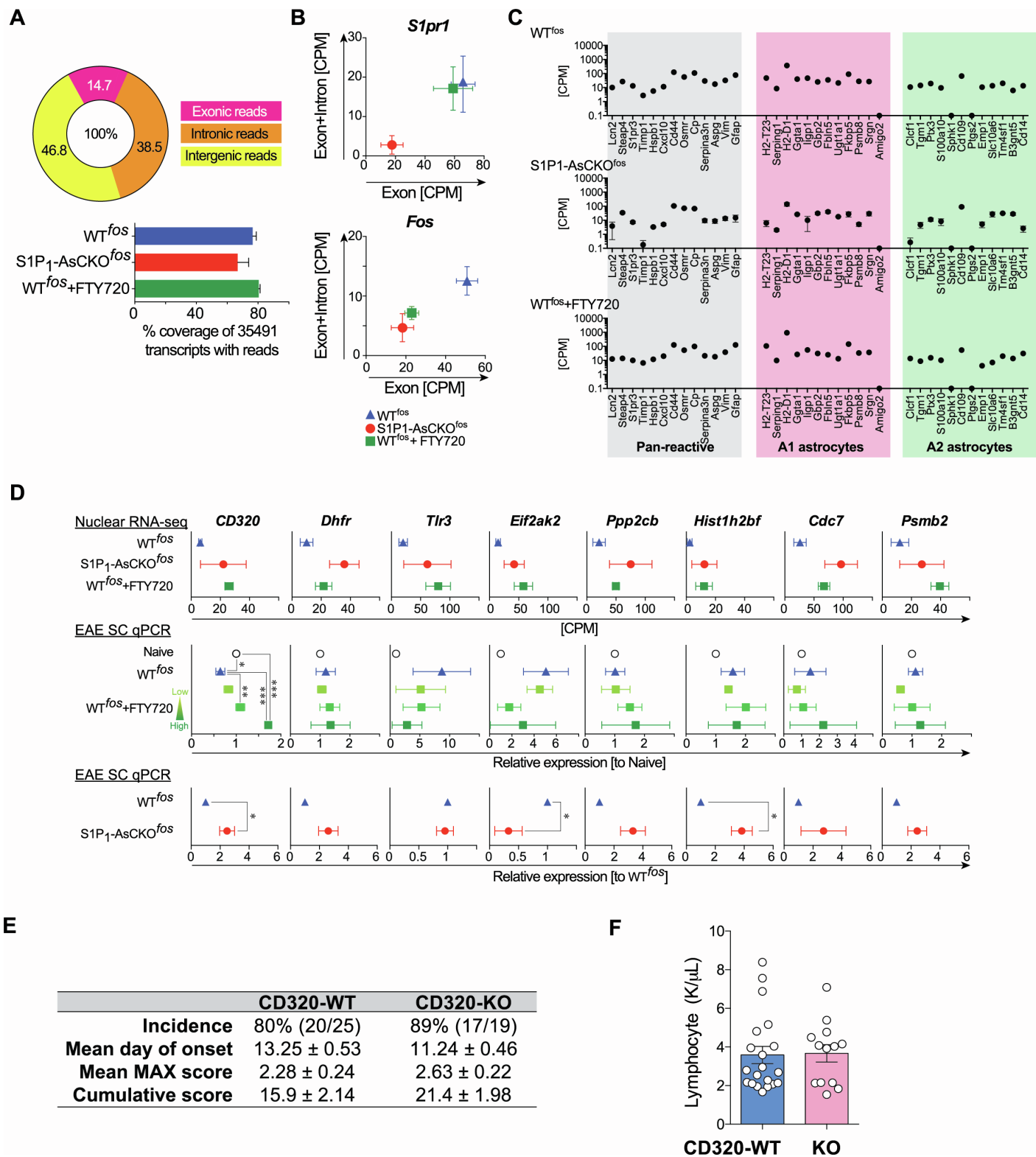


Fig. S1. snRNA-seq and CD320 identification.

A, averaged percentage of exonic, intronic, and intergenic reads in nuclear RNA-seq. The percent of reads that mapped to exons and introns were uniquely characteristic of nuclear RNA, with an increased representation of intronic reads. Percent coverage of transcripts (mean ± SEM). **B**, the exonic and exonic+intronic reads of

Slpr1 were diminished only in S1P₁-AsCKO^{fos} when compared to WT^{fos} and WT^{fos}+FTY720, indicating that the DAPI⁺NeuN⁻GFP⁺ nuclei were derived from astrocytes. The exonic and exonic+intronic reads of *fos* were diminished in both S1P₁-AsCKO^{fos} and WT^{fos}+FTY720, indicating less astrocytic activation in these mice. **C**, comparison between nuclear RNA-seq data vs. recently proposed Pan/A1/A2 reactive astrocyte-specific genes. Although there was no obvious A1/A2-skewing² in DAPI⁺NeuN⁻GFP⁺ populations, more than 90% of reactive astrocyte-specific genes were detected. **D**, expression profile of 8 genes identified in the pathway analysis that correspond to **Fig. 1 C** (mean ± SEM, *, p < 0.05; **, p < 0.01; *** p < 0.001 by one-way ANOVA in FTY720 groups, and one sample t test in KO groups). **E**, clinical parameters of EAE in CD320-WT and CD320-KO mice. Composite data from three independent experiments are shown. Cumulative scores were the sum of clinical scores from days 0 to 20 (means ± SEM, * p < 0.05 by Mann-Whitney U test). **F**, peripheral lymphocyte numbers. Each circle represents a single animal (mean ± SEM).

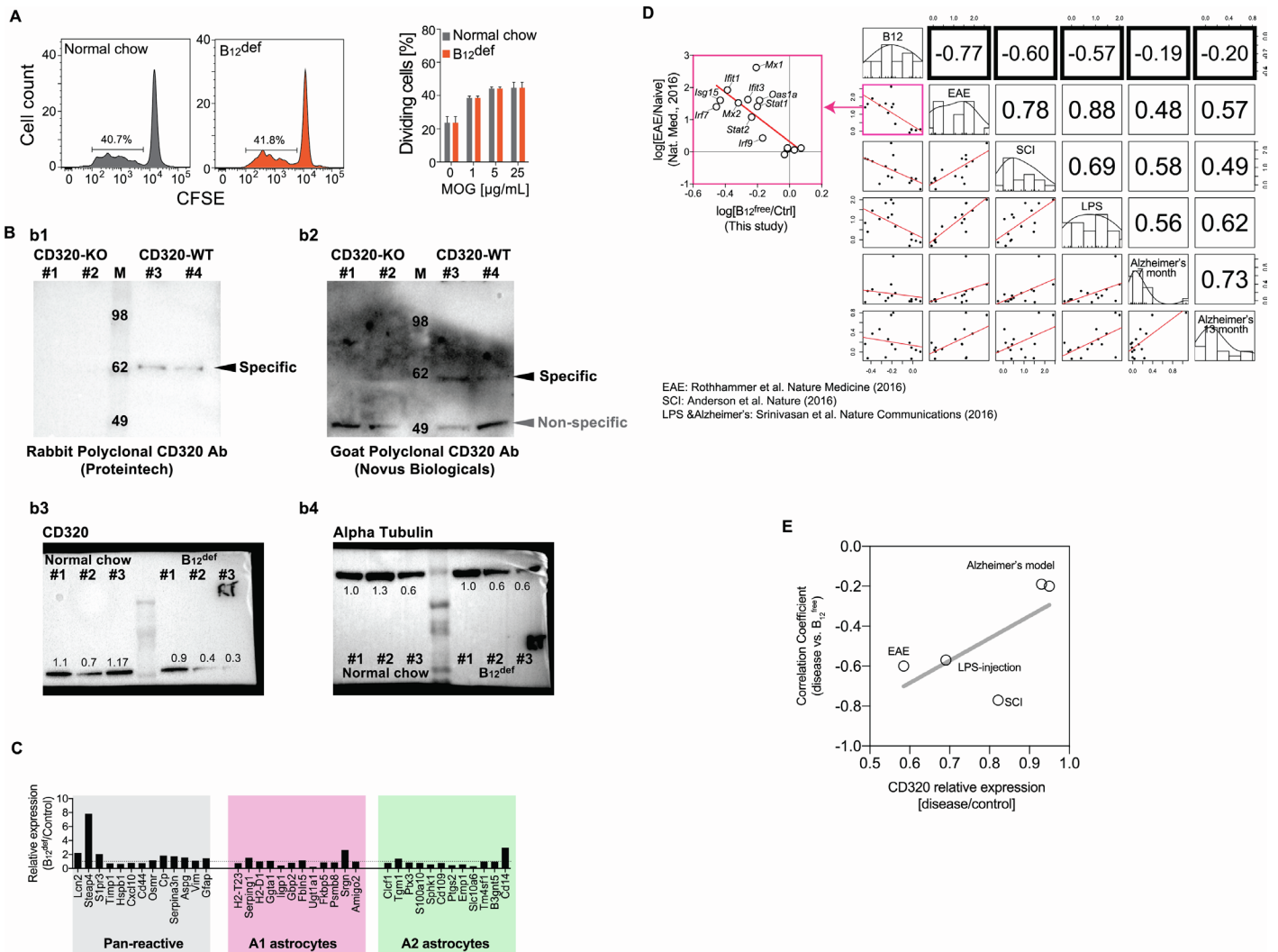


Fig. S2. Analyses of B₁₂^{def} EAE mice and B₁₂^{free} astrocytes.

A, T cell proliferation. Mononuclear cells were isolated from spleens of MOG₃₅₋₅₅ immunized mice, and cultured in the presence or absence of MOG₃₅₋₅₅ for three days. Representative histograms of carboxyfluorescein succinimidyl ester (CFSE) intensities of CD3⁺ T cells are shown from two independent experiments. Percentage of dividing T cells is indicated. MOG-induced cell proliferation is comparable in B₁₂^{def} vs. controls (mean ± SEM, n = 3). **B**, Western blotting for CD320. (b1 and b2) Antibody specificities were assessed using proteins extracted from CD320-WT and CD320-KO SCs. The specific bands observed in CD320-WT disappeared in CD320-KO, indicating that both antibodies showed high specificity against mouse CD320. The calculated mass of CD320 is 27.7 kDa, but it is a heavily glycosylated protein³. (b3 and b4) CD320 expression was suppressed in EAE-induced B₁₂^{def} mice as compared with controls. Numbers indicate relative intensities. **C**, Comparison between astrocyte RNA-seq data vs. recently proposed Pan/A1/A2 reactive astrocyte specific genes. No obvious A1/A2-skewing² was observed in B₁₂^{def} astrocytes. **D**, Correlation matrix. Numbers indicate correlation coefficients. Correlation analyses of astrocytic IFN-I gene expression changes showed negative correlations between B₁₂^{free} (B₁₂-free astrocyte culture) vs. EAE⁴, SC injury⁵, and LPS-injected mice⁶, but no correlation was found between B₁₂^{free} vs. Alzheimer's model mice⁶. **E**, correlation of CD320 fold changes vs. correlation coefficients between B₁₂^{free} (bold boxes in D) and indicated disease conditions. Moreover, these correlation coefficients were positively correlated with the extent of astrocytic Cd320 down-regulation in these diseases, suggesting an association of astrocytic IFN-I sensitivity with the B₁₂-CD320 pathway in neuroinflammation.

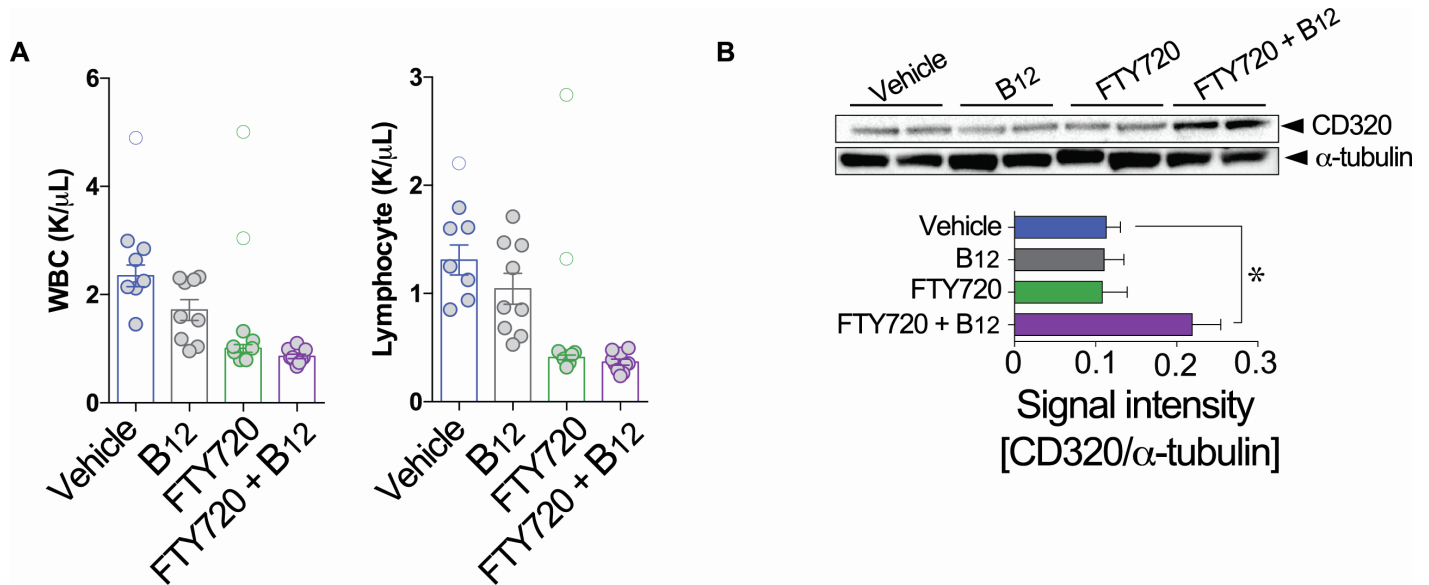


Fig. S3. FTY720 efficacy in B_{12}^{def} mice.

A, peripheral white blood cell (WBC) and lymphocyte counts in EAE mice treated with vehicle, B_{12} , FTY720, and FTY720+ B_{12} . Lymphocyte trafficking effects of FTY720 appear to be intact for all experimental conditions examined. Each point represents a single animal. Some samples (open circles) were eliminated from the datasets based on Smirnov-Grubbs test before performing statistical analysis by Kruskal-Wallis test with Dunn's multiple comparisons test (mean \pm SEM). **B**, Western blotting for CD320 in SCs of EAE mice at 50 days post immunization (dpi) and 25 days post treatment from 25 dpi. Signal intensity of CD320 was normalized by comparison to α -tubulin (mean \pm SEM, $n = 4$ animals, * $p < 0.05$ by one-way ANOVA with Bonferroni's multiple comparisons test).

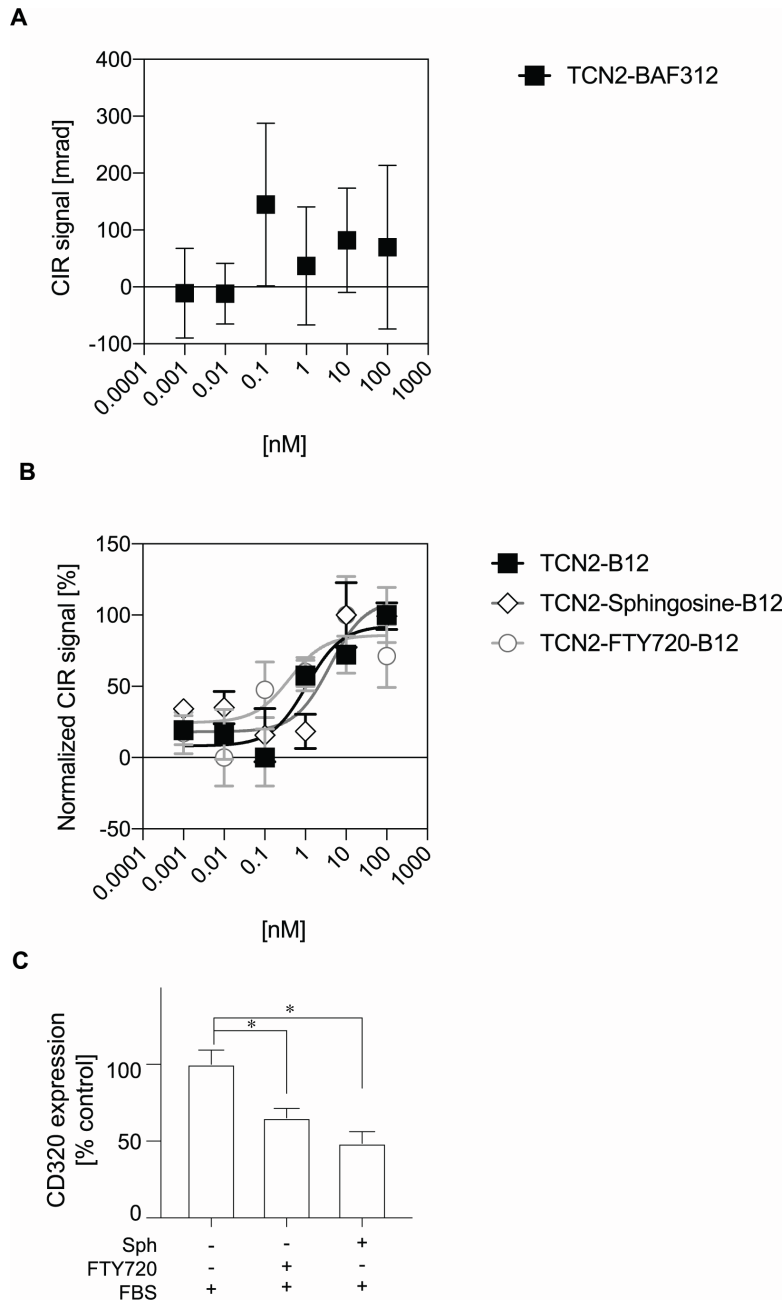


Fig. S4. Compensated interferometric reader (CIR)-based binding assay and CD320 internalization. A, No clear binding signals between TCN2 vs. BAF312 (siponimod). **B,** Specific binding curves between TCN2-B₁₂ (K_d = 5.98 ± 8.96 nM) vs. FTY720 (K_d = 5.62 ± 5.24 nM) and sphingosine (K_d = 0.33 ± 0.33 nM). Compensated Interferometric Reader (CIR) signals are plotted against concentrations of binding partners, normalized, and fitted by nonlinear regression using the Michaelis-Menten equation (mean ± SEM, n = 4-5, p = 0.34 by One-way ANOVA). **C,** CD320 internalization in HASTR/ci37 cells. Cells were stimulated with 1 μM FTY720 or 1 μM Sph in the presence of FBS. * p < 0.05, one-way ANOVA with Bonferroni's multiple

comparisons test.

References

1. Fabregat, A., Sidiropoulos, K., Viteri, G., Forner, O., Marin-Garcia, P., Arnau, V., D'Eustachio, P., Stein, L., and Hermjakob, H. (2017). Reactome pathway analysis: a high-performance in-memory approach. *BMC Bioinformatics* *18*, 142. 10.1186/s12859-017-1559-2.
2. Liddelow, S.A., Guttenplan, K.A., Clarke, L.E., Bennett, F.C., Bohlen, C.J., Schirmer, L., Bennett, M.L., Munch, A.E., Chung, W.S., Peterson, T.C., et al. (2017). Neurotoxic reactive astrocytes are induced by activated microglia. *Nature* *541*, 481-487. 10.1038/nature21029.
3. Quadros, E.V., and Sequeira, J.M. (2013). Cellular uptake of cobalamin: transcobalamin and the TCblR/CD320 receptor. *Biochimie* *95*, 1008-1018. 10.1016/j.biochi.2013.02.004.
4. Rothhammer, V., MSCANFRONI, I.D., Bunse, L., Takenaka, M.C., Kenison, J.E., Mayo, L., Chao, C.C., Patel, B., Yan, R., Blain, M., et al. (2016). Type I interferons and microbial metabolites of tryptophan modulate astrocyte activity and central nervous system inflammation via the aryl hydrocarbon receptor. *Nat Med* *22*, 586-597. 10.1038/nm.4106.
5. Anderson, M.A., Burda, J.E., Ren, Y., Ao, Y., O'Shea, T.M., Kawaguchi, R., Coppola, G., Khakh, B.S., Deming, T.J., and Sofroniew, M.V. (2016). Astrocyte scar formation aids central nervous system axon regeneration. *Nature* *532*, 195-200. 10.1038/nature17623.
6. Srinivasan, K., Friedman, B.A., Larson, J.L., Lauffer, B.E., Goldstein, L.D., Appling, L.L., Borneo, J., Poon, C., Ho, T., Cai, F., et al. (2016). Untangling the brain's neuroinflammatory and neurodegenerative transcriptional responses. *Nat Commun* *7*, 11295. 10.1038/ncomms11295.